The impact of β-myrcene – the main component of the hop essential oil – on the lipid films

Karolina Połeć, Marcin Broniatowski, Paweł Wydro, Katarzyna Hąc-Wydro *

Faculty of Chemistry, Jagiellonian University, Gronostajowa 2, 30-387 Kraków, Poland

A B S T R A C T

β-myrcene (myrcene) is the main component of the hop essential oil, the latter being a plant derived extract of a wide range of antimicrobial properties. To get a deeper insight in the role of myrcene in the membrane-related activity of the total extract, in this work the effect of this terpene on the lipid monolayers was investigated. The aim of the studies was to analyze and to compare the influence of myrcene on the one component films formed by the lipids typical of plant and fungi membranes and differing in the structure of both polar and non-polar part of the molecule. The experiments involved the surface pressure-area measurements, the penetration and the relaxation studies, Brewster angle microcopy and Grazing incidence X-ray diffraction (GIXD) studies. It was found that myrcene causes the decrease of the condensation and/or stability and changes the morphology of the lipid monolayers, however its exact effect is determined by the concentration and by the lipid type. Moreover, the mechanisms leading to the alterations within the organization of the film are different depending on the monolayer material and they may involve the extraction of the molecules from the interface and/or accommodation of terpene in the lipid environment. It was also summarized that although myrcene and the hop essential oil affect the properties of the lipid films they act on the studied membranes according to different mechanisms.

© 2020 The Authors. Published by Elsevier B.V. This is an open access article under the CC BY license (http://creativecommons.org/licenses/by/4.0/).

1. Introduction

The essential oils and their particular components are known from a wide range of their biological activities. For many of them, antibacterial or/and antifungal properties were confirmed; some of them act as a non-toxic anti-angiogenic and anticancer agents and their antioxidant properties were also postulated [1–3]. All the mentioned above activities predestine these chemicals to be used as natural, ecological or "green" therapeutics, preservatives, food additives or pesticides.

As in the case of all of the bioactive substances, the practical use of the essential oils should be preceded by a thorough studies leading to the exploration of various aspects of their activity. For example, it is extremely important to select the compound(s), which are responsible for biological effects exerted by the studied plant extract. Moreover, the recognition of the mechanisms of the activity/selectivity and the identification of the possible side effects of the chemicals are also vital. As it was reported in literature (e.g. Refs. [4,5]), the essential oils are able to induce their therapeutic effect by the acting at different levels of the cells. In the other words, there is no one specific target in cells responsible for the activity of these substances. However, what is common for these chemicals, the active molecules have to overcome the barrier of

the cellular membrane to reach the target in the cell interior. It is also highly important that the penetration of the oil components into the membrane or their diffusion through the lipid bilayer may lead to significant perturbations in the membrane organization. The latter can be the important part of a complex mechanism of action of the compound or even the basis for its biological activity or toxicity [6,7]. Therefore, the investigations on the effect of the essential oils and their particular components on membranes is very important step in the investigations on their properties and the areas of their applications.

The studies on the mechanism of action and the membrane activity of both bio-molecules and xenobiotic are comprehensive and systematic and they are performed both on natural cells/membranes and on the artificial systems [8,9]. The application of the model lipid systems seems to be a good starting point in these researches. A lower complexity of model membranes and the ability of the researcher to fix the composition and physicochemical parameters of the system as well as to control the external conditions during experiments allow one to collect the information on the behavior of the studied substance in the membrane-like environment [10,11]. For example, based on the obtained results it is possible to conclude on the affinity of the extract or its components to membrane, analyze the penetration abilities of the compound, select the phytocompound of the strongest effect on membrane organization or indicate the lipid(s) of special importance from the point of view of the membrane-activity of the investigated substance.

* Corresponding author.
  E-mail address: hac@chemia.uj.edu.pl (K. Hąc-Wydro).

Recently, we have started in our laboratory the investigations on the antibacterial effect of the hop essential oil [12]. The experiments were performed on the ternary model lipid system (monolayers and bilayers) imitating plant pathogen bacteria membrane as well as on its particular lipid components. It was found that the studied plant extract components easily incorporate into the membranes and the whole mixture acts as a fluidizing agent. However, the effect of the hop oil increases only up to a given concentration and the further increase of the extract concentration does not strengthen the observed effects. Our results on model systems together with the results of the in vitro test allowed one to draw conclusion that the hop essential oil affects membrane organization and reveals antibacterial activity. Thus, it could be applied for example as the natural pesticide.

However, it is not known, which of the component of the hop oil is decisive from the point of view of the extract activity. During our analysis of the hop extract composition, β-myrcene (myrcene, 7-methyl-3-methylideneocta-1,6-diene) was recognized as the main component of the mixture [12]. This compound is a monoterpene, which derives its name from *Myrcia* species forming a large flowering plant family [13]. Based on the detailed verification of the absorption, metabolism and excretion of myrcene in humans as well as taking into account that myrcene is used in low doses, and it is lack of significant genotoxic and mutagenic potential, this compound has the status: "generally recognized as safe" (GRAS). Therefore, it is widely used as a fragrance in cosmetics, anti-odour agent, cleaning products and as the food additive [14,15]. Myrcene is also highly important raw material for the production of various naturally occurring compounds used as flavors, fragrances, cosmetics, vitamins, and pharmaceuticals or pheromones [14,16]. Although myrcene is naturally produced by various plants, its direct extraction is uneconomical. However, industrially it can be easily obtained via pyrolysis of β-pinene, the latter being a key compound of the turpentine (that is the volatile compounds of crude balsams from conifers, mainly from the *Pinaceae* family) [14].The production of myrcene in microbial synthesis via metabolically engineered *Escherichia coli* was also reported [14]. Microbiological studies evidenced the antibacterial properties of myrcene on *Staphylococcus aureus*, *Escherichia coli*, *Salmonella enterica* [17] as well as on plant pathogenic bacteria *Agrobacterium tumefaciens* and *Erwinia carotovora* var. *carotovora* [18]. Moreover, the ability of myrcene to locate in the cellular membranes was reported [19,20]. All the foregoing facts may suggest that this compound is responsible for the membrane-fluidizing activity of the hop essential oil as well as its antibacterial effect. Therefore, the aim of this work is to investigate the effect of myrcene on one component insoluble monolayers formed by the lipids typical for bacteria and fungi membranes. To perform systematic investigations the lipids selected differ in the structure of polar head as well as in the saturation degree of the apolar part of the molecule.

2. Experimental

2.1. Materials

The lipids investigated in this work, namely: 1-palmitoyl-2-oleoyl-*sn*-glycero-3-phosphoethanolamine (POPE), 1,2-dipalmitoyl-sn-glycero-3-phosphoethanolamine (DPPE), 1-palmitoyl-2-oleoyl-*sn*-glycero-3-phospho-(1′-rac-glycerol) (sodium salt) (POPG), 1,2-dipalmitoyl-sn-glycero-3-phospho-(1′-rac-glycerol) (sodium salt) (DPPG), 1′,3′-bis[1,2-dioleoyl-*sn*-glycero-3-phospho]-*sn*-glycerol sodium salt (C:18 Cardiolipin, TOCL), 1,2-dipalmitoyl-*sn*-glycero-3-phosphocholine (DPPC) and 1-palmitoyl-2-oleoyl-*sn*-glycero-3-phosphocholine (POPC), were the synthetic compounds of high purity (≥99%) purchased from Avanti Polar Lipids Inc., USA. These lipids were dissolved in a chloroform/methanol (9:1 v/v) mixture (HPLC grade, ≥99.9%, Aldrich). The studied terpene, β-myrcene (myrcene), was supplied by Sigma Aldrich. The stock solutions of myrcene were prepared in a high purity ethanol (HPLC grade, ≥99.9%, Aldrich).

2.2. Methods

2.2.1. Surface pressure–area measurements

The surface pressure (π)–area (A) isotherms were recorded for the monolayers formed from particular lipids on water subphase and on myrcene solutions. The solutions of terpene were prepared by the dilution of the stock solution prepared in ethanol (the concentration 0.1 mol/dm^3) in Ultrapure Milli-Q water to obtain the solutions of the following concentrations: 0.49; 0.73; 0.98; 1.22 and 13.6 μg/ml (which corresponds to the concentrations range from $3.5 \cdot 10^{-6}$ to $1 \cdot 10^{-4}$ M). These concentrations correspond to those used in our previously done experiments on the effect of the hop essential oil on the lipid monolayers [12]). The myrcene solutions were used on the day of their preparation. To form the monolayers, the respective lipid solutions were deposited onto the subphase (pure water or myrcene solutions) with the Hamilton micro syringe (±1.0 μl). Then, the monolayers were left for 5 min before the compression was started with the barrier speed of 10 cm^2/min. These experiments were done on KSV-NIMA Langmuir trough (total area = 275 cm^2) having two Delrin barriers enabling symmetrical compression of the monolayers. The trough was placed on an anti-vibration table. The surface pressure was measured (±0.1 mN/m) with the Wilhelmy plate made of filter paper (ashless Whatman Chr1) connected to the electrobalance. The experiments were done at 20 °C and the subphase temperature was controlled thermostatically (±0.1 °C) by a circulating water system. The measurements were repeated at least twice to obtain consistent results (the error for the area per molecule does not exceed 0.2 Å^2/molecule).

Based on the obtained results, the compressional modulus values were calculated according to Eq. 1:

$$C_S^{-1} = -A(d\pi/dA) \tag{1}$$

wherein A is the mean area per molecule value at a given surface pressure π. The higher C_S^{-1} values the lower lateral elasticity of model membrane [21].

To compare the effect of myrcene on the position of the isotherm the changes in the area per molecule values in respect to the values on water subphase at different surface pressures were calculated.

2.2.2. Penetration experiments

The studies on the penetration of myrcene into the lipid films were done in a following procedure. The lipid monolayer was prepared on water subphase and compressed up to the target surface pressure and then left for equilibration to desirable initial surface pressure π_i ($\pi_i = 10$ and 30 mN/m). Then, the myrcene solution prepared in ethanol was injected into the subphase to the final concentration 13.6 μg/ml. After the injection, the increase of the surface pressure (at a constant area), caused by the incorporation of the terpene into the lipid film, was monitored up to the constant value (equilibrium surface pressure — π_{eq}) or per ca. 1 h. During experiments, the subphase was continuously stirred. As it was found in preliminary experiments, the injection of sole ethanol into the subphase (in the volume corresponding to the volume of ethanolic extract solutions introduced during penetration experiments) does not alter the surface pressure. Thus, the observed changes in π values were induced only by the presence of myrcene. The results of these experiments, namely, the changes in the surface pressure to constant values (π_{eq}), were analyzed in respect to the initial surface pressure (π_i). Thus, $\Delta\pi_{eq}$ values ($\Delta\pi_{eq} = \pi_{eq} - \pi_i$) were calculated and analyzed. The penetration is the stronger the higher $\Delta\pi_{eq}$ value. The positive values of this parameter ($\Delta\pi_{eq}$) means that myrcene molecules incorporate into the monolayer and accommodate within the lipid molecules. On the other hand, $\Delta\pi_{eq} \approx 0$ means that terpene molecules are excluded from the interface, while $\Delta\pi_{eq} < 0$ evidences destabilization of the film and possible dragging of the molecules into the bulk phase.

2.2.3. Stability measurements

The monolayers formed by particular lipids on myrcene solution (concentration 13.6 μg/ml) were compressed to the surface pressure 30 mN/m and then, after the barriers were stopped, the changes of the area per molecule values in time were monitored. A decrease of the relative area in time means desorption of the molecules from the interface. Thus, to gain some insight into the desorption process occurring for the studied herein systems the model proposed by Ter Minassian-Saraga [22] was applied. According to the latter model, the desorption process may involve two steps: the dissolution and then the diffusion. In the consequence of the dissolution into the bulk phase the saturated layer under the surface is formed and the rate of this step of desorption can be calculated from Eq. (2):

$$- \log\frac{A}{A_0} = k_1 t^{\frac{1}{2}} \tag{2}$$

where k_1 is the rate of dissolution, A is the area occupied at time t, while A_0 is an initial area at $t = 0$.

The second step of desorption, namely the diffusion of the molecules from the formed sublayer, may occur when the desorption achieves a steady-state. The rate of this process can be calculated based on Eq. (3):

$$- \log\frac{A}{A_0} = k_2 t \tag{3}$$

where k_2 is the rate of diffusion.

The fitting of the linear curve(s) to the linear part(s) of $- \log\frac{A}{A_0}$ vs $t^{\frac{1}{2}}$ and $- \log\frac{A}{A_0}$ vs t plots allows one to calculate, from the slopes of the fitted curves, the rates of particular steps of the relaxation process. It should be however stressed that sometimes the mechanism of the relaxation of the film is complicated and during this process, the steady state is not reached. In the latter situation the relaxation involves more than one dissolution steps of different rates.

2.2.4. Brewster angle microscopy studies

The morphology of the monolayers formed on water and on the myrcene solution (of the concentration 13.6 μg/ml) was analyzed in Brewster angle microscopy experiments. In these experiments, an UltraBAM instrument (Accurion GmbH, Goettingen, Germany) equipped with a 50-mW laser emitting p-polarized light at a wavelength of 658 nm, a 10× magnification objective, polarizer, analyzer and a CCD camera was used. The spatial resolution of the microscope was 2 μm. The foregoing apparatus and the Langmuir trough were placed on the table (Standa Ltd., Vilnius, Lithuania) equipped with an active vibration isolation system (antivibration system VarioBasic 40, Halcyonics, Göttingen, Germany).

2.2.5. Grazing incidence X-ray diffraction (GIXD)

The experiments were performed on the SIRIUS beamline at SOLEIL synchrotron (Gif-sur- Yvette, France) using the dedicated liquid surface diffractometer. The detailed construction of the diffractometer working at the SIRIUS beamline and the parameters of the synchrotron beam applied in the GIXD experiments are described on the SOLEIL web site (www.synchrotron-soleil.fr) and in our previous papers [23,24] whereas the foundations of the technique are summarized in the excellent review articles [25,26]. The GIXD studies were performed for DPPE, DPPC and DPPG monolayers on water and on myrcene solutions of the highest concentrations (13.6 μg/ml).

3. Results

3.1. The influence of myrcene on POPE,POPE, POPC and TOCL monolayers

The surface pressure–area curves (π–A isotherms) for POPE, POPC, POPG and TOCl monolayers spread on water and on the solutions of myrcene of different concentrations were shown in Fig. 1a–d. In Fig. 2a–d, the compressional modulus vs the surface pressure plots for the films on water and on the myrcene solutions of the highest concentrations are shown. As it is seen for POPE and POPG monolayers, the effect of myrcene depends on its concentration in the subphase. Namely, with the increasing content of myrcene, the isotherms shift to the larger areas and they change their slope. For POPC and TOCl films, the latter effect is observed only at the highest concentration of terpene in the solution. Moreover, for POPC the isotherm changes its slop and, at higher surface pressures, it is situated even at lower areas than the curve for the film on water. The effect of myrcene reflects also in a decrease of the compressional modulus values for the studied films. The first conclusion obtained from these results is that myrcene affects the condensation of the studied monolayers and the ordering of the molecules at the interface.

To facilitate the analysis and presentation of the collected data leading to the comparison of the results for particular monolayers more deeply, further presentation of the calculated parameters was limited to those obtained for the highest concentration of myrcene in the subphase. Thus, the shift, in percent, of the isotherm at two different (namely low and high) surface pressures were determined and presented in Fig. 3. In the same figure, the results of the penetration experiments performed at two different initial surface pressures (10 and 30 mN/m) were shown as the Δπ vs time plots.

The analysis of the surface pressure–area curves evidenced that the shift of the curves at the highest content of myrcene in the subphase is very comparable for POPE and POPG films, and much lower for TOCl, both at low and high surface pressure (Fig. 3).

A drop of the maximal values of the compressional modulus values, which indicates a decrease of the ordering of the molecules at the interface (Fig. 2) changes in the following order: POPE (ca. 41%), POPG (ca. 28%) and TOCl (ca. 21%). Interestingly, at lower surface pressures, myrcene practically does not change the compressional modulus for POPE. On the other hand, myrcene causes the shift of the transition surface pressure existing for POPE monolayer to the higher π values. The latter means that terpene prevents POPE molecules from the formation of the condensed phase at the interface and in this sense, myrcene affects POPE films even at lower π values. Moreover, the results of penetration experiments (Fig. 3) indicate that at lower π the injection of myrcene solution causes the increase of the surface pressure, thus myrcene molecules incorporate into POPE monolayer. The penetration data for POPG and TOCL indicate that $\Delta\pi_{eq} \leq 0$, both at low and high surface pressures. Thus, initially the molecules of terpene insert into these monolayers, however, they easily escape form the interface to the bulk phase. Moreover, the decrease of the surface pressure below the initial value ($\Delta\pi eq < 0$) (without film stabilization) may suggest that also the monolayer material is partially removed from the interface or dragged into the subphase.

In Fig. 4, the BAM images taken for POPE monolayers are shown. As it can be seen, at the surface pressures above the transition surface pressure, the monolayer on myrcene solution is less condensed, which reflects in a lower number of the condensed domains, which additionally do not merge up to the collapse the latter being in contrast to the film on water. Thus, although the penetration experiments do not evidence that myrcene incorporates into the surface film, the terpene molecules affect the monolayer morphology.

The trends in the effect of myrcene on POPC isotherms are different from those found for the remaining lipid films. Although myrcene affects these films only at the highest applied concentration, the isotherm changes drastically its slope and, at higher surface pressures, it is shifted
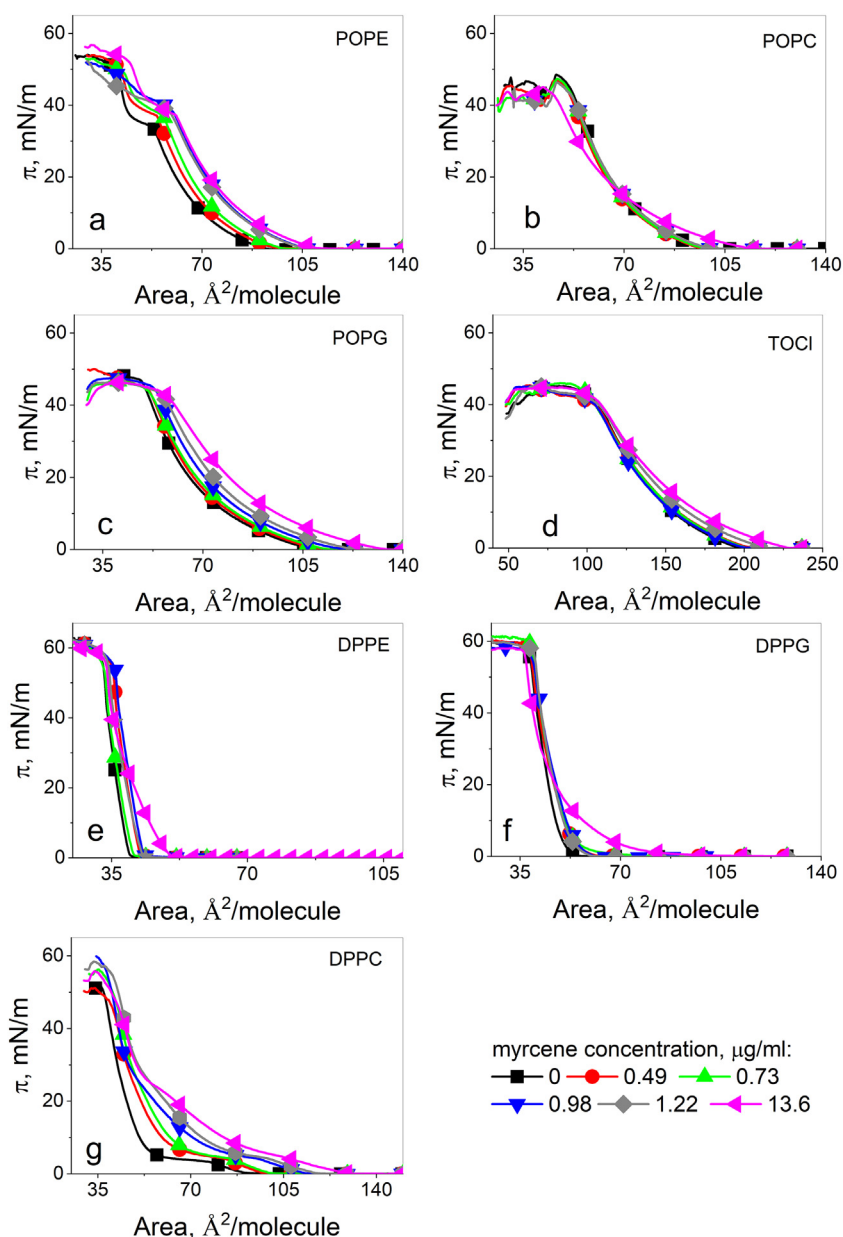
Fig. 1. The surface pressure-area isotherms for the studied lipid monolayers spread on water and on myrcene solutions of different concentrations.

to the lower areas as compared to the curve on water. The latter reflects in the negative values of ΔA for POPC film (Fig. 3). This phenomenon can be attributed to the exclusion of the monolayer material from the interface to the bulk phase. Moreover, terpene molecules only slightly penetrate the POPC film (slightly positive values of Δπeq).The influence of myrcene reflects also in a pronounced decrease of the compressional modulus values (ca. 31%).

To verify more deeply the stability of particular monolayers in the presence of myrcene, the changes in the area per lipid in time, at π = 30 mN/m, were monitored. The results of these experiments are shown in Fig. 3. It is known that the phospholipid monolayers formed at the air/water interface are highly stable, and the relative area (A/A₀) values, after a small decrease at the beginning of the measurements, remain constant at least during 1 h of monitoring. This relates both to the fully saturated as well as to the unsaturated phospholipids (e.g. Ref. [27]). As is can be found in Fig. 3 the stability of the films analyzed in this paragraph decreases as follows: TOCL > POPC > POPE > POPG. It can be also easily noticed that the relative area does not drop in time

monotonically but in the A/A₀ vs time plots the regions of different slopes can be easily noticed. Considering the procedure of the performed experiments, it is clear that a drop of the area at a constant surface pressure is the consequence of the removal of the molecules from the interface or rather their dragging deeply into the bulk phase. To discuss the relaxation of the monolayer and possible desorption process of the molecules from the interface the model proposed by Ter Minassian-Saraga [22] was applied. According to the procedure described in the experimental section the rates of dissolution and diffusion (two steps of desorption process assumed in the above model) for the studied monolayers in the presence of myrcene were calculated. The results of these calculations are presented in Table 1, while the examples of the curves fitted to the experimental data are shown in Supplementary Materials (Fig. S1).

For all the investigated monolayers, it was impossible to fit the linear curve to the results obtained at the initial stage of the measurements, which is the expected phenomenon caused by the reorientation of the molecules at the interface. Among the discussed in this paragraph,
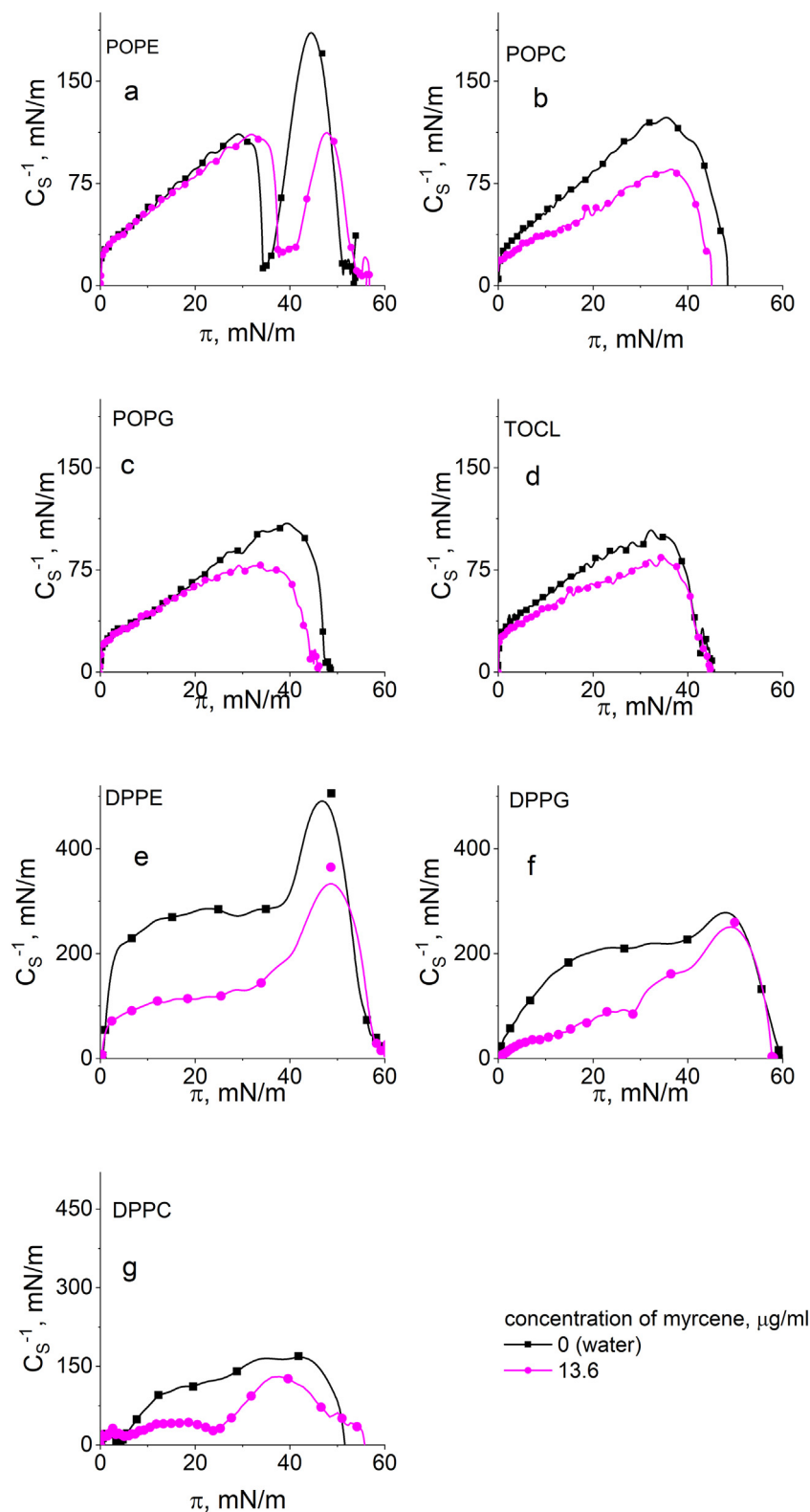
Fig. 2. The compressional modulus values vs the surface pressure plots for the lipid monolayers on water and on myrcene solution.

phospholipids only for TOCl monolayer the steady state between dissolution and diffusion steps of relaxation is reached. For POPC and POPG films, the dissolution is controlled by three different constant rates. However, this process is faster for POPG than for POPC. For POPE monolayer, the situation is even more complicated. Namely, to the data obtained during ca. 39 min of the experiments two dissolutions processes controlled by two different constant rates was found. However, then the relative area values practically do not change, which indicates that the monolayer is stable. However, after further 12 min. The A/A_0 values start to decrease, thus the desorption process is continued.
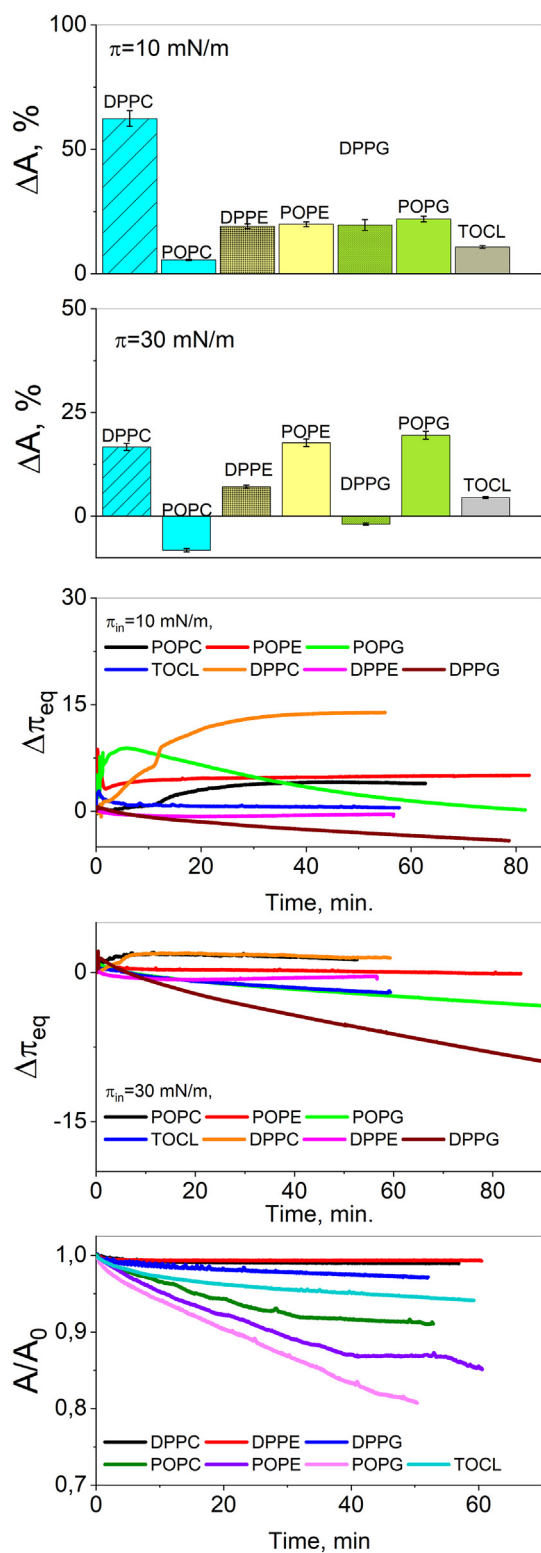
Fig. 3. The shift of the isotherms (ΔA, in percent) caused by the presence of myrcene in the subphase, the results of penetration experiments for the investigated lipid film at different surface pressures (concentration of myrcene: 10^{-4} M) and the results of the stability measurements (The A/A_0 vs time plots for the lipid film on myrcene solution).

3.2. The influence of myrcene on DPPE, DPPC and DPPG monolayers

The results of the surface pressure-area measurements for the phospholipids having two fully saturated C16:0 chains area presented in

Fig. 1e–g. Among the monolayers formed by the saturated lipids only for those composed of DPPC molecules, the dependency between the myrcene concentration and the isotherms position was found. Namely, the isotherm shifts to the larger areas and the LE/LC phase transition is also shifted to the higher values. For DPPC films, both at high and at low surface pressures, the influence of myrcene on the position of the isotherm is visibly stronger as compared to its effect of DPPE and DPPG (Fig. 3). It was also found that the ordering of monolayer formed by the saturated lipids (DPPC, DPPG and DPPE) is more strongly affected by myrcene than the ordering of the remaining studied lipids. This is reflected in the pronounced decrease of the compressional modulus values (Fig. 2). Thus, the effect of myrcene on the organization of highly ordered films formed by DPPC, DPPE and DPPG is more strongly reflected in the compressional modulus values as compared to the influence on their saturated-unsaturated counterparts. It could be suggested that a denser packing of the molecules at the interface facilitates the membrane-disturbing activity of myrcene. This conclusion seems to be in accordance with the discussed above results obtained for POPE monolayers. Namely, for POPE film the visible decrease in C_S^{-1} occurs only above the transition surface pressures, when the domains of the condensed phase are formed. Moreover, the decrease of this parameter, measured in percent, is comparable for DPPC, DPPE and DPPG.

Interestingly, at 30 mN/m, myrcene causes some shift of the curve for DPPG to the lower areas. This effect may indicate that in the presence of myrcene the molecules are in part eliminated from the interface. A further interesting finding is the additional kink appearing in the isotherms for DPPC and DPPG monolayers spread in the presence of myrcene. This effect can be well detected in the C_S^{-1} vs π dependencies since the kinks in the isotherms manifest as the small minima in the foregoing plots. The existence of the kink in the surface pressure–area curve may also suggest the removal of myrcene molecules from the interface, with the monolayer compression.

The results of penetration studies for these monolayers (Fig. 3) evidenced that only for DPPC film, both at low and high initial surface pressure, after the injection of terpene solution the surface pressure increases and in time achieves a stable positive values ($\Delta\pi_{eq}$). For the remaining phospholipids (DPPE, DPPG), $\Delta\pi_{eq}$ values are ca. zero or they drop below zero even at lower initial surface pressure. Thus, myrcene molecules tend to be removed from the interface and additionally this process may involve the dragging of the lipid molecules into the bulk phase. The latter suggestion in respect to DPPG seems to be additionally conformed by a well observed shift of the isotherm to the areas lower than those for the film on water.

Based on the results presented in Table 1 and Fig. 3, it can be found that DPPC and DPPE monolayers compressed in the presence of myrcene are highly stable. Namely, after the initial molecular rearrangements of the monolayer the area values do not change with time during ca. 1 h of measurements. For DPPG the decrease of the relative area is observed, however, it is much smaller as compared to that found for previously discussed TOCL, POPC, POPE, POPG films. Moreover, the relaxation of DPPG monolayer in the presence of myrcene consists of two dissolution steps, without achieving a steady state. However, the constant rates for these steps are much lower than those for the remaining monolayers.

BAM images taken for the monolayers formed by fully saturated phospholipids on water and on myrcene solutions are shown in Fig. 4. As it can be seen for DPPC films, the effect of myrcene on the morphology of the monolayer is highly manifested both at low and high surface pressures. In short, in the presence of terpene, the domains of the condensed phase are formed at higher surface pressures and they are much smaller and of different morphology as compared to those observed on pure water. The molecules of DPPE and DPPG form at the air/water interface highly ordered films and the large patches of the condensed phase are easily observed even at low surface pressures. The presence of myrcene in the subphase does not cause substantial alterations in the morphology of these films at high π values. However, at
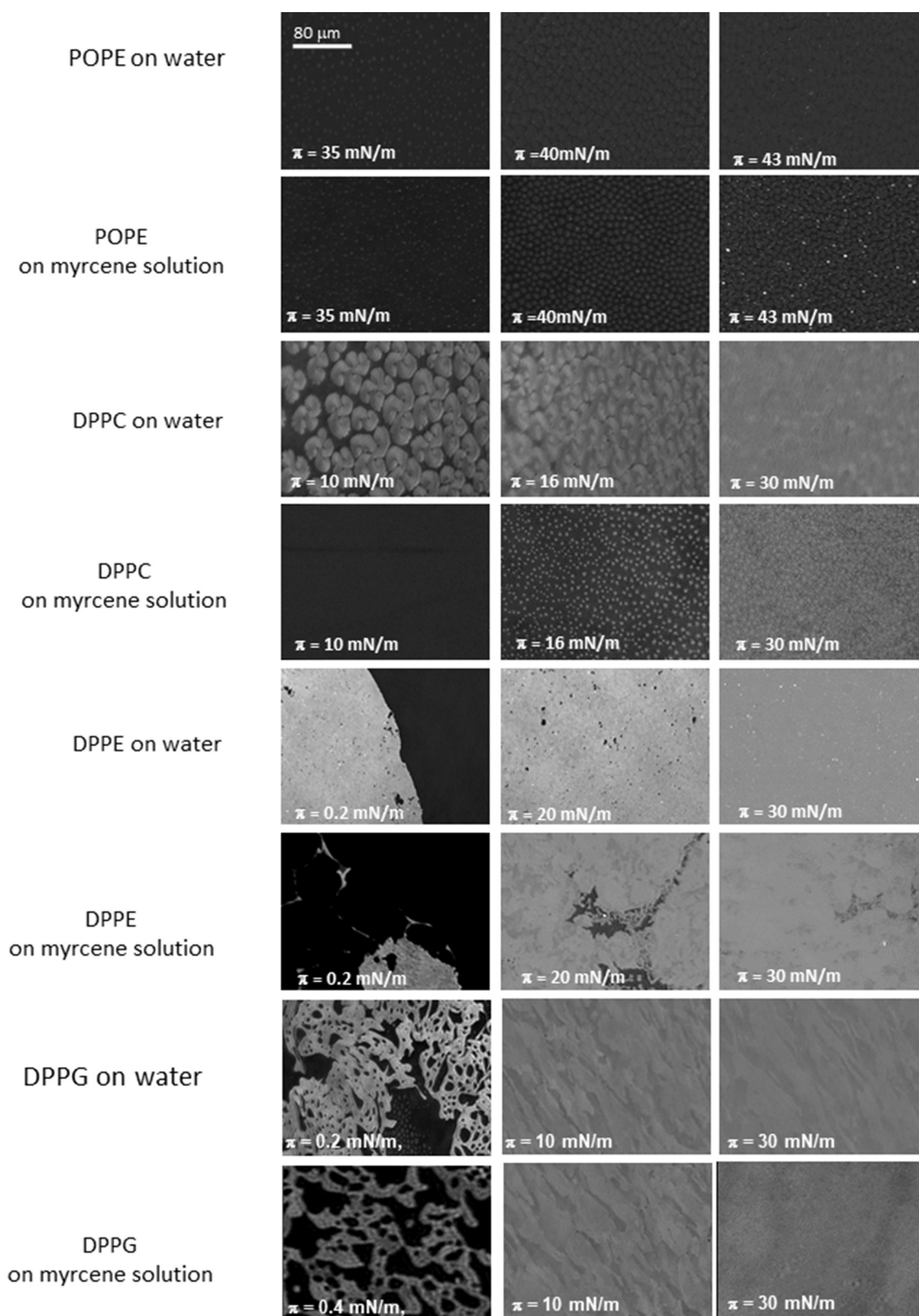
Fig. 4. BAM images for the lipid films on water and in the presence of myrcene in the subphase.

the beginning of the compression (at low surface pressures) both monolayers are less condensed.

The compilation of these results allows one to draw conclusion that myrcene incorporates into DPPC films and significantly changes its molecular organization both at low and high surface pressures. On the other hand, the effect of myrcene on DPPE and DPPG monolayer is significantly less manifested in the results of the performed experiments. However, for these highly ordered phospholipid films it was possible to perform also GIXD experiments, which provide the information on the molecular organization of the surface and the effect of myrcene on

Table 1
The rate of dissolution (k_1, k_1', k_1'') and diffusion k_2 together with the R-square (R) for the lipid monolayer in the presence of myrcene in the subphase. For POPE film, the calculations involve first 40 min of the measurements.

	$k_1 \cdot 10^{-3}$/R [1/min$^{-1/2}$]	$k_1' \cdot 10^{-3}$/R [1/min$^{-1/2}$]	$k_1'' \cdot 10^{-3}$/R [1/min$^{-1/2}$]	$k_2 \cdot 10^{-3}$/R [1/min]
DPPG	2.05 ± 0.01/0.999	1.63 ± 0.01/0.999	–	–
POPG	9.91 ± 0.02/0.999	14.8 ± 0.03/0.999	20.9 ± 0.05/0.999	–
TOCL	4.10 ± 0.01/0.998	–	–	0.235 ± 0.005/0.997
POPC	5.19 ± 0.01/0.999	8.57 ± 0.01/0.999	2.27 ± 0.01/0.999	–
POPE	10.71 ± 0.01/0.999	14.82 ± 0.01/0.999	–	–

the ordering of hydrophobic chains at the nanometer scale. As it was reported in multiple publications, the monolayers of DPPE [28–30], DPPG [30–33] and DPPC [31,34] are 2D crystalline, that is they diffract constructively X-ray synchrotron radiation and can be successfully investigated with the application of Grazing Incidence X-ray Diffraction (GIXD) method. Thus, the application of the model membranes constructed of dipalmitoyl phospholipids enables the studies of the effects exerted by bioactive molecules, as myrcene in these studies, on the packing mode of the phospholipid molecules within the 2D crystalline lattice with molecular resolution. Myrcene is a small and flat hydrocarbon molecule, the structure of which resembles the terminal part (acyl chain) of the membrane steroids (the structure of myrcene molecule is presented in a Graphical abstract, TOC). Therefore, when myrcene migrates from the aqueous solution it can pack in the voids between the palmitoyl chains and change their orientation at the air/water interface. The packing mode of DPPE, DPPG and DPPC is not the same at a given surface pressure value as the tilt of the palmitoyl chains and its orientation in the monolayer plane depends on the size and chemical properties of the polar headgroup. Therefore, it is possible that the effects of myrcene incorporation can differ depending on the headgroup type. To shed light on these interesting questions and verify the effects exerted of myrcene on DPPE, DPPG and DPPC monolayers at 15 and 30 mN/m the GIXD experiments were performed. The results for DPPE are presented in Figs. 5 and 6, while for DPPG at 30 mN/m in Fig. 7. The results for DPPG at 15 mN/m and all the results for DPPC were directed to Supplementary Materials (Figs. S2, S3) due to the reasons specified in the text. All the structural parameters calculated from the GIXD data are gathered in Table 2.

DPPE has a small headgroup which is moderately hydrated due to the limited tendency of the —NH$_3^+$ of the terminal ethanolamine moiety to hydrogen bond formation. At higher surface pressures (30 mN/m), the palmitoyl chains are tightly packed (solid state of the monolayer) and oriented parallel to the monolayer normal, so their packing mode can be described by the hexagonal 2D crystal lattice [29,30]. At 15 mN/m, the monolayer is in the liquid-condensed state with the palmitoyl chains tilted collectively ($\tau = 18.8$) from the monolayer normal; thus, the symmetry of the 2D lattice is lowered (rectangular centered). The data obtained for DPPE monolayer on the aqueous subphase is in accordance with scientific literature [28–30].

At 15 mN/m, in the presence of myrcene in the subphase, three separate diffraction signals are visible in the intensity map (Fig. 5b). Therefore, three separate Bragg peaks and Bragg rods were calculated from these data and indexed with the Miller h,k indices $\langle 0,1 \rangle$, $\langle 1, \rangle$ and $\langle -1,1 \rangle$. Three separate diffraction signals are typical to the oblique 2D lattice [25,26]. The $\langle -1,1 \rangle$ signal has its intensity maximum close to the horizon; whereas the $\langle 0,1 \rangle$ and $\langle 1,0 \rangle$ signals have their intensity maxima shifted much over the horizon to higher Q_z values. The tilt angle τ in the presence of myrcene is increased only slightly to 20.2°, so the change in the packing mode of the palmitoyl chains is connected with the alteration of the tilt azimuth from the nearest neighbor (NN) to the intermediate orientation. In the rectangular centered and oblique lattices, the ordering parameter L_{xy} is anisotropic and depends on the crystallographic direction. However, in the presence of myrcene the increase of L_{xy} in all the directions can be observed. L_{xy} is especially high (614 Å) in the $\langle -1,1 \rangle$ direction analogous to the $\langle 0,2 \rangle$ direction in the rectangular centered lattice, for which the value of 197 Å was calculated. Therefore, it can be concluded that at 15 mN/m some myrcene molecules are incorporated between the DPPE palmitoyl chains and they exert a rather organizing effect leading to the three-fold increase of the 2D crystallinity range. For the DPPE monolayer compressed to
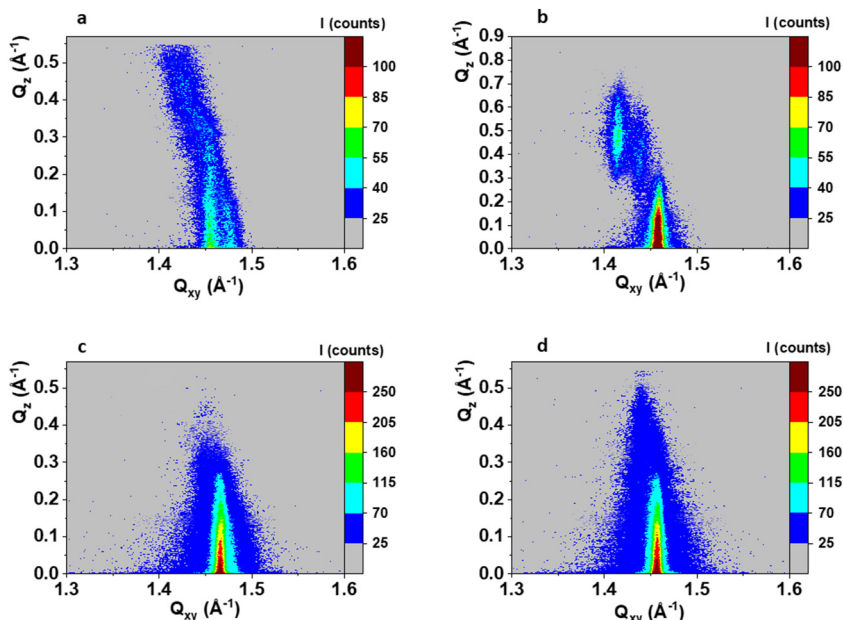

Fig. 5. Intensity maps I(Q_{xy},Q_z) for the DPPE monolayers: a) 15 mN/m water, b) 15 mN/m myrcene solution, c) 30 mN/m water, d) 30 mN/m myrcene solution.
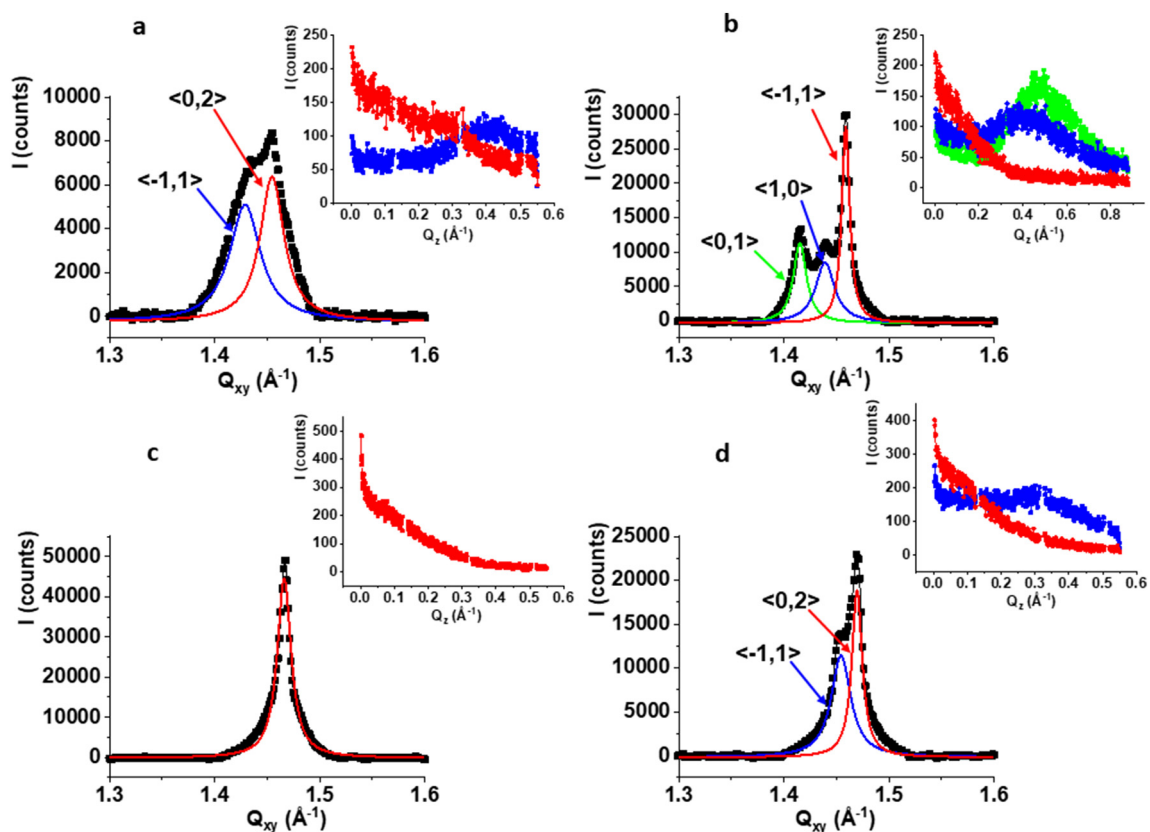
Fig. 6. Bragg peak I(Q$_{xy}$) and Bragg rod I(Q$_z$) profiles calculated from the intensity map I(Q$_{xy}$,Q$_z$) for the DPPE monolayers: a) 15 mN/m water, b) 15 mN/m myrcene solution, c) 30 mN/m water, d) 30 mN/m myrcene solution. The green, blue and red lines are Lorentz curve fits to the experimental data. The Bragg rods are calculated for the specified maxima.
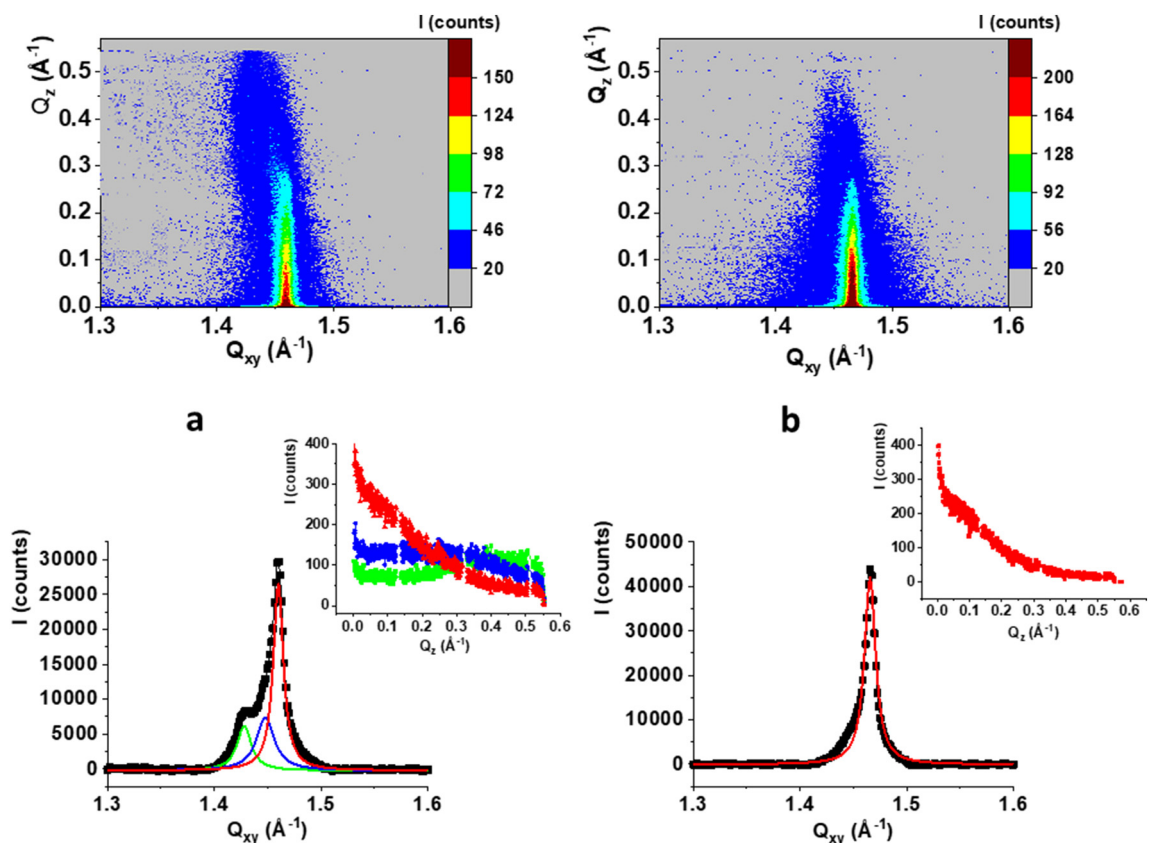

Fig. 7. GIXD data: intensity map I(Q$_{xy}$,Q$_z$), Bragg peak and Bragg rod profiles collected at π = 30 mN/m for the DPPG monolayers spread on: a) pure water, b) myrcene solution.

Table 2
Structural parameters calculated from the GIXD data: Q_{xy} — location of the intensity maximum of the diffraction signal, Q_z — location of the intensity maximum of Bragg rod; a, b, γ — the lattice parameters, L_{xy} — the range of 2D crystallinity, A — area of the unit cell (per one hydrocarbon chain), τ — tilt angle.

System	Q_{xy}, Å⁻¹	Q_z, Å⁻¹	a, b, Å, Å, γ, °	A, Å²	L_{xy}, Å	τ, °
DPPE, water, π = 15 mN/m	<−1,1> 1.429 <0,2> 1.454	<−1,1> 0.42 <0,2> 0	5.107, 8.643, 90	44.1	<−1,1> 154 <0,2> 197	18.8
DPPE, myrcene, π = 15 mN/m	<0,1> 1.415 <1,0> 1.439 <−1,1> 1.459	<0,1> 0.50 <1,0> 0.38 <−1,1> 0.006	4.969, 5.054 118.52	22.1	<0,1> 368 <1,0> 251 <−1,1> 614	20.2
DPPE water, π = 30 mN/m	1.466	0	4.949	21.2	346	0
DPPE myrcene, π = 30 mN/m	<−1,1> 1.454 <0,2> 1.469	<−1,1> 0.30 <1,0> 0	5.007, 8.554, 90	42.8	<−1,1> 244 <0,2> 464	13.4
DPPG water, π = 15 mN/m	<0,1> 1.390 <1,0> 1.424 <−1,1> 1.449	<0,1> 0.60 <1,0> 0.48 <−1,1> 0.054	4.998, 5.121, 118.0	22.6	<0,1> 204 <1,0> 168 <−1,1> 503	24.4
DPPG myrcene, π = 15 mN/m	<0,1> 1.403 <1,0> 1.430 <−1,1> 1.454	<0,1> 0.59 <1,0> 0.40 <−1,1> 0.050	4.988 5.084, 118.2	22.3	<0,1> 276 <1,0> 204 <−1,1> 614	23.2
DPPG water, π = 30 mN/m	<−0,1> 1.428 <1,0> 1.448 <−1,1> 1.460	<0,1> 0.40 <1,0> 0.20 <−1,1> 0.045	4.961, 5.030, 119.0	21.8	<0,1> 345 <1,0> 276 <−1,1> 461	15.6
DPPG myrcene, π = 30 mN/m	1.465	0	4.953	21.2	435	0
DPPC water, π = 15 mN/m	<−1,1> 1.301 <0,2> 1.430	<−1,1> 0.84 <0,2> 0	5.782, 8.788, 90	50.8	<−1,1> 146 <0,2> 553	37.7
DPPC myrcene, π = 15 mN/m	<−1,1> 1.305 <0,2> 1.433	<−1,1> 0.82 <0,2> 0	5.561, 8.769, 90	50.5	<−1,1> 142 <0,2> 512	36.9
DPPC water, π = 30 mN/m	<0,1> 1.386 <1,0> 1.415 <−1,1> 1.449	<0,1> 0.60 <1,0> 0.45 <−1,1> 0.08	5.015, 5.120, 117.71	22.7	<0,1> 118 <1,0> 104 <−1,1> 553	24.2
DPPC myrcene, π = 30 mN/m	<0,1> 1.347 <1,0> 1.407 <−1,1> 1.436	0.73 0.46 0.06	5.020, 5.244 117.19	23.4	<0,1> 102 <1,0> 63 <−1,1> 291	28.7

30 mN/m on the pure aqueous solution only one diffraction signal can be observed in the intensity map; whereas in the presence of myrcene two signals are visible — the first with it intensity maximum at $Q_z = 0$ Å⁻¹ and the second with its intensity maximum at $Q_z = 0.30$ Å⁻¹. This alteration corroborates the presence of some myrcene molecules incorporated between the palmitoyl chains also in these experimental conditions. Myrcene incorporated to the monolayer induces the tilt of the palmitoyl chains from the monolayer normal (τ = 13.4); thus, the physical state of the monolayer changes from solid (water) to liquid — condensed (myrcene). This is in accordance with significant lowering of the compression modulus observed for DPPE monolayer spread on the myrcene solution (compare with Fig. 2). Therefore, at the surface pressure of 30 mN/m, the effect of myrcene incorporation can be classified as disorganizing. On the other hand, the incorporation of myrcene does not affect the range of 2D crystallinity within the investigated monolayer, which is even higher in the presence of myrcene (464 Å) than on pure water (346 Å).

In the subsequent GIXD experiments, the effects of myrcene incorporation to DPPG monolayer were investigated. As it can be compared in Table 2, the results obtained at 15 mN/m for the monolayers spread on pure water and on myrcene solution were practically identical. In both the cases, the packing of the palmitoyl chains can be described by the oblique lattice; thus, the intensity maps, Bragg peaks and Bragg rods are presented in the Supplementary Materials (Fig. S2). Significant differences between the monolayers were noticed at π = 30 mN/m, so the GIXD data collected in these experimental conditions are presented in Fig. 7.

At first glance there are two diffraction signals in the I(Q_{xy},Q_z) plot registered for the DPPG monolayer spread on pure water — one with its intensity maximum at $Q_z = 0$ and the second at $Q_z > 0$, which indicates the rectangular centered lattice with the NN azimuth. However, the thorough analysis of the Bragg rods enables the identification of two closely located and partially overlapped signals with intensity maximum at $Q_z = 0.40$ (0,1) and $Q_z = 0.20$ (1,0) defining the oblique lattice

similarly to the measurements performed at 15 mN/m. These data are in agreement with our previous paper [30] in which the GIXD data for DPPG monolayers were collected on a different synchrotron facility (BW1, Hasylab, Hamburg). The compression of the monolayer from 15 to 30 mN/m reduces the tilt angle τ from 24.4 to 15.6° but the monolayer still remains in the liquid-condensed state, which is in agreement with the compressional modulus plots (Fig. 2). At 30 mN/m, the presence of myrcene molecules between the palmitoyl chains changes profoundly their orientation at the air/water interface, as they are oriented perpendicularly with the tilt angle τ reduced to 0. This can be inferred from the I(Q_{xy},Q_z) plot at which only one diffraction signal with the intensity maximum at $Q_z = 0$ Å⁻¹ can be observed. In the presence of myrcene, the 2D lattice is now hexagonal. The thorough analysis of the Bragg rod profiles this time does not allow to discern any other signals, overlapped or merged in the I(Q_{xy},Q_z) image; thus the presence of myrcene exerts this time an organizing effect on the orientation of the palmitoyl chains at the interface. As it was mentioned above, the orientation of the acyl chains in the monolayer is governed by the size and hydration of the polar headgroup. The phosphatidylglycerol (PG) molecule has a larger headgroup than PE, and the terminal glycerol molecule can form effective hydrogen bonds with water molecules which increases the hydration and by this the effective size of the headgroup. Thus, the packing of the palmitoyl chains is less tight than in the case of DPPE. The migration of the myrcene molecules within the hydrophobic environment of the hydrocarbon chains should be easier and more effective in the case of DPPG than DPPE monolayer. As the palmitoyl chains of DPPG are less ordered than in the case of DPPE there is the room for the ordering action of small hydrophobic molecules well fit to voids between the chains. The palmitoyl chains are the effective scatterers, which diffract the X-ray radiation. We usually tend to approximate the whole hydrophobic chain as a rigid rod; however, due to thermal oscillation the terminal parts can be disordered or the gauche defects can break the rods [35]. Therefore, the effective scatterer can be shorter than ¹⁶C atoms and the tilt effect can be caused not by the

inclination of the whole palmitoyl chain as a rigid rod but by the disorder of its terminal part. The presence of myrcene in the DPPG monolayer can limit the oscillations of the terminal parts of the palmitoyl chains and by this eliminate the tilt effects leading finally to the hexagonal ordering of the scatterers. The proposed here model is illustrated in the Graphical Abstract (TOC).

Finally, the GIXD experiments were performed for DPPC monolayers. At 15 mN/m, the diffraction signal can be already measured but its intensity is low. One diffraction signal is located at $Q_z = 0$ Å^{-1}, and the second very high above the horizon, at $Q_z > 0.8$ Å^{-1}. The second signal is weak and diffused — probably it is a superposition of two separate signals and the 2D lattice should be described as oblique; however, the quality of the Bragg rod profiles is here very low; thus the 2D lattice was approximated as rectangular centered with a large tilt of the palmitoyl chains $\tau = 37.7^o$. In the presence of myrcene the GIXD data were practically identical. The compression of the monolayer to 30 mN/m increased the intensity of the diffraction signal and improved its quality. This time it was possible to discern three separate signals and define the oblique lattice well known for this phospholipid from literature [31,34]. Again, the presence of myrcene does not lead to any significant changes of the palmitoyl chains ordering. The GIXD data – Bragg peak and Bragg rod profiles for the DPPC monolayers – are presented in Supporting Materials in Fig. S3. Thus, it can be concluded that the presence of myrcene between the hydrocarbon chains in the DPPC monolayer is quite neutral for the chain ordering. Again, it can be explained by the size of the polar headgroup. The phosphatidylcholine headgroup is the largest among the double-chained phospholipids. The charged —N(CH$_3$)$_3^+$ choline groups does not form hydrogen bonds with each other but due to the partial positive charge are well hydrated. The large head-group prevents the chains from high ordering, so the voids between the chains are larger than in the DPPE and DPPG monolayers.

4. Discussion

The collected results allow one to summarize that myrcene molecules may lead to the decrease of the condensation and/or stability of the investigated lipid monolayers as well as to change their morphology. The alterations in the properties of the surface films caused by the investigated terpene were detected for all the studied herein lipids, however their magnitude was different depending on the lipid type, the surface pressure and terpene concentration. Moreover, the collected results suggest also that myrcene acts on the studied lipid monolayers according to different mechanisms, which may include the extraction of the molecules from the interface and/or accommodation of terpene in the lipid environment.

First of all, it was found that the effect of myrcene on DPPC, POPE and POPG monolayers depends on the terpene concentration, which is in contrast to the remaining films affected only at the highest terpene content in the subphase. This allows one to conclude that DPPC, POPE and POPG films are more susceptible to the myrcene influence than DPPG, DPPE, TOCL and POPC monolayers. Moreover, at the highest concentration of myrcene and at lower surface pressures, all the monolayers become more expanded (the shift of the isotherms to larger areas, the alterations in BAM pictures) and this effect is the most pronounced for DPPC films. However, as result from the penetration experiments at 10 mN/m, terpene molecules are able to accommodate in some extend only within DPPC, POPE and POPC films. As indicated the data obtained for the remaining films, myrcene molecules tend to be rather removed from the interface. However, even in the latter situation, they are still able to affect the film organization.

From the point of view of the discussion of the effect of biomolecules on membranes, the results obtained in the monolayer experiments performed at high surface pressure region are more important. The results collected at these conditions for POPE monolayer evidence strong effect of myrcene on the film fluidity and morphology, which reflects in the position of the isotherms, in the decrease of the

compressional modulus values and in BAM images. Since myrcene does not penetrate the monolayer at high surface pressure region, it seems that its effect is based on the destabilization of the film. Vey similar conclusions on the effect of myrcene at higher surface pressures can be drawn for POPG and TOCL films. Namely, the increase of the monolayer fluidity and its strong gradual destabilization were confirmed during analysis of the isotherm position, compressional modulus values and stability measurements. Similarly to POPE films, myrcene does not penetrate TOCL and POPG monolayers, and after initial incorporation, the terpene molecules are removed from the interface. The analysis of the data resulting from stability measurements suggests that in the presence of myrcene the monolayer material is removed or partially dragged into the bulk phase. Among these three phospholipids, the effect of myrcene is the strongest on POPE and the weakest on TOCl films.

As far as phosphatidylcholine (PC) monolayers are concerned, the collected results allow one to propose that the mechanism of action of myrcene on POPC vs DPPC films is different. First of all, for POPC monolayer, a noticeable effect of myrcene appears only at the highest applied concentration, while for DPPC the shift of the isotherms even at the lowest applied terpene concentration was noticed. In this sense, POPC film is less affected by the terpene than DPPC monolayers. Secondly, the penetration experiments evidenced that myrcene molecules are able to incorporate into both DPPC and POPC films thus phosphatidylcholine lipids ensure the most convenient environment for terpene accommodation. However, the terpene causes strong destabilization of POPC monolayers by a gradual dissolution of the monolayer. The ability of myrcene to extract POPC molecules from the monolayer reflects directly in the shape and position of the isotherm recorded on myrcene solution. The latter effect was not found for DPPC film. On the other hand, in the case of DPPC myrcene does not cause desorption of the monolayer material from the interface (the film is highly stable), but rather incorporates within the lipids environment. Moreover, the results of GIXD experiments performed on DPPC monolayers confirm that myrcene molecules localized within the lipid molecules at the interface do not affect the chain ordering. However, all the obtained results confirm that the terpene causes strong modification of the condensation and morphology of DPPC monolayer. It seems that the condensed domains formed at the interface facilitate the accommodation of myrcene molecules leading to the fluidization of the monolayer.

The remaining studied herein fully saturated phospholipids, namely DPPE and DPPG form at the air/water interface the monolayers of even the higher condensation than DPPC. However, although the decrease of the ordering of the molecules at the interface measured by the drop of the compressional modulus values for all the saturated lipids is very similar, the effect of the terpene on DPPE and DPPG monolayers is not reflected in the collected experimental results as significantly as for DPPC. Firstly, for DPPE and DPPG, the effect of myrcene can be noticed only at the highest content of the terpene in the subphase. Moreover, for DPPG, at 30 mN/m, myrcene causes some shift of the curve to the lower areas. This fact together with the results of the stability measurements and penetration studies suggests that in the presence of myrcene the molecules are in part eliminated from the interface, however the desorption occurs in a lower extend as compared to the remaining monolayers. Although the GIXD data suggest that myrcene molecules tend to order the terminal parts of the phospholipid chains the overall effect of myrcene on DPPG film results in the monolayer fluidization.

For DPPE film, the fluidizing influence of myrcene reflects only in the shift of the isotherm to larger area and in the decrease of the compressional modulus. The monolayer is highly stable and the penetration results do not reflect incorporation of the terpene into the monolayer. However, the analysis of the properties of the hydrophobic part of the molecules in a nanoscale by GIXD studies confirm that both at low and high surface pressure some myrcene molecules are incorporated between the DPPE palmitoyl chains. The analysis of GIXD data provide

the conclusion that myrcene molecules cause the tilt of the palmitoyl chains from the monolayer normal decreasing significantly the physical state of the film.

Recently, the effect of the hop essential oil on POPE, POPG and TOCL monolayers was investigated [12] at the same conditions as those applied in this work. Comparing the results obtained at higher surface pressure region, for the hop essential oil, which is the mixture of different terpenes, with the results obtained for myrcene, which is the main component of the hop essential oil, the following conclusions can be drawn. Both the essential oil and myrcene affect POPG and POPE films in the concentration dependent way. However, the components of the hop essential oil are systematically removed from the interface with these films compression. The latter effect was not observed in the isotherms recorded for POPE, POPG and TOCL films spread on myrcene solution. This may explain the fact that myrcene causes stronger shift of the isotherms at a given surface pressure and concentration than the hop oil. The latter effect is especially pronounced for POPE and POPG films. Namely, the shift, ΔA [%] of the isotherms at $\pi = 30$ mN/m caused by myrcene is 16.4 and 12.3 for POPE and POPG, while it is 5.0 and 6.4 for the hop essential oil. However, as it was evidenced [12], the components of the hop essential oil easily penetrate all the foregoing monolayer and after injection into the film they accommodate within the lipid molecules. The mechanism of action of myrcene seems to be different. Namely, the results obtained for myrcene evidenced that this terpene is not able to penetrate POPE, POPG and TOCL films at high surface pressure; however, terpene causes strong destabilization of these films by the desorption of the monolayer material from the interface. Although both myrcene and the hop extract decreases condensation of the lipid monolayers, the fluidizing effect seems to be achieved according to different mechanisms. It can be summarized that although myrcene is the main component of the hop essential oil [12] and it causes strong alterations in membrane properties, this molecule acts on the studied membranes in a different wat than the hop essential oil. In this sense, myrcene does not determine the effect of total mixture on the discussed phospholipids.

Declaration of competing interests

The authors declare that they have no known competing financial interests or personal relationships that could have appeared to influence the work reported in this paper.

CRediT authorship contribution statement

Karolina Połeć: Validation, Investigation, Formal analysis, Visualization, Writing - original draft, Writing - review & editing.**Marcin Broniatowski:** Validation, Investigation, Formal analysis, Visualization, Writing - original draft, Writing - review & editing.**Paweł Wydro:**Validation, Investigation, Writing - original draft, Writing - review & editing.**Katarzyna Hąc-Wydro:**Conceptualization, Methodology, Writing - original draft, Writing - review & editing, Formal analysis, Visualization, Supervision.

Appendix A. Supplementary data

Supplementary data to this article can be found online at https://doi. org/10.1016/j.molliq.2020.113028.

References

[1] K.A. Hammer, C.F. Carson, T.V. Riley, Antimicrobial activity of essential oils and other plant extracts, J. Appl. Microbiol. 86 (1999) 985–990, https://doi.org/10.1046/j.1365-2672.1999.00780.x.

[2] U. Sitara, I. Niaz, J. Naseem, N. Sultana, Antifungal effects of essential oils on in vitro growth of pathogenic fungi, Pak. J. Bot. 40 (1) (2008) 409–414.

[3] G. Nieto, Biological activities of three essential oils of the Lamiaceae family, Medicines 4 (2017) https://doi.org/10.3390/medicines4030063E63; 10 pages.

[4] H. Tsuchiya, Membrane interactions of phytochemicals as their molecular mechanism applicable to the discovery of drug leads from plants, Molecules 20 (2015) 18923–18966, https://doi.org/10.3390/molecules201018923.

[5] S. Chouhan, K. Sharma, S. Guleria, Antimicrobial activity of some essential oils—present status and future perspectives, Medicines 4 (E58) (2017) https://doi.org/10.3390/medicines403005821 pages.

[6] A. Bouyahya, J. Abrini, N. Dakka, Y. Bakri, Essential oils of *Origanum compactum* increase membrane permeability, disturb cell membrane integrity, and suppress quorum sensing phenotype in bacteria, J. Pharm. Anal. 9 (2019) 301–311, https://doi.org/10.1016/j.jpha.2019.03.001.

[7] M. Carvalho, H. Albano, P. Teixeira, In vitro antimicrobial activities of various essential oils against pathogenic and spoilage microorganisms, J. Food Qual. Hazards Control 5 (2018) 41–48, https://doi.org/10.29252/jfqhc.5.2.3.

[8] A. Maćczak, P. Duchnowicz, P. Sicińska, M. Koter-Michalak, B. Bukowska, J. Michałowicz, The in vitro comparative study of the effect of BPA, BPS, BPF and BPAF on human erythrocyte membrane; perturbations in membrane fluidity, alterations in conformational state and damage to proteins, changes in ATP level and Na +/K+ ATPase and AChE activities, Food Chem. Toxicol. 110 (2017) 351–359, https://doi.org/10.1016/j.fct.2017.10.028.

[9] K. Olechowska, M. Mach, K. Hąc-Wydro, P. Wydro, Studies on the interactions of 2-hydroxyoleic acid with monolayers and bilayers containing cationic lipid: searching for the formulations for more efficient drug delivery to cancer cells, Langmuir 35 (2019) 9084–9092, https://doi.org/10.1021/acs.langmuir.9b01326.

[10] K. Hąc-Wydro, P. Dynarowicz-Łątka, Biomedical applications of the Langmuir monolayer technique, Annales Universitatis Mariae Curie-Skłodowska 4 (2008) 47–60, https://doi.org/10.2478/v10063-008-0027-2Lublin-Polonia, sectio AA chemia, LXIII.

[11] Ch. Peetla, A. Stine, V. Labhasetwar, Biophysical interactions with model lipid membranes: applications in drug discovery and drug delivery, Mol. Pharm. 6 (2009) 1264–1276, https://doi.org/10.1021/mp9000662.

[12] K. Połeć, B. Barnaś, M. Kowalska, M. Dymek, R. Rachwalik, E.a Sikora, A. Biela, M. Kobiałk, K. Wójcik, K. Hąc-Wydro The influence of the essential oil extracted from hops on monolayers and bilayers imitating plant pathogen bacteria membranes, Colloids Surf. B: Biointerfaces 173 (2019) 672–680, doi:https://doi.org/10.1016/j.colsurfb.2018.10.047.

[13] M.M. Cascaes, G.M. Skelding Pinheiro Guilhon, E.H. de Aguiar Andrade, M. das Graças Bichara Zoghbi, L. da Silva Santos, Constituents and pharmacological activities of *Myrcia* (Myrtaceae): a review of an aromatic and medicinal group of plants, Int. J. Mol. Sci. 16 (2015) 23881–23904, https://doi.org/10.3390/ijms161023881.

[14] A. Behr, L. Johnen, Myrcene as a natural base chemical in sustainable chemistry: a critical review, ChemSusChem 2 (2009) 1072–1095, https://doi.org/10.1002/cssc.200900186.

[15] T.B. Adams, C. Lucas Gavin, M.M. McGowen, W.J. Waddell, S.M. Cohen, V.J. Feron, L.J. Marnett, I.C. Munro, P.S. Portoghese, I.M.C.M. Rietjens, R.L. Smith, The FEMA GRAS assessment of aliphatic and aromatic terpene hydrocarbons used as flavor ingredients, Food Chem. Toxicol. 49 (2011) 2471–2494, https://doi.org/10.1016/j.fct.2011.06.011.

[16] E.M. Kim, J.H. Eom, Y. Um, Y. Kim, H.M. Woo, Microbial synthesis of myrcene by metabolically engineered *Escherichia coli*, J. Agric. Food Chem. 63 (18) (2015) 4606–4612, https://doi.org/10.1021/acs.jafc.5b01334.

[17] Ch.-Y. Wang, Y.-W. Chen, Ch-Y. Hou, Antioxidant and antibacterial activity of seven predominant terpenoids, Int. J. Food Prop. 22 (1) (2019) 230–238, https://doi.org/10.1080/10942912.2019.1582541.

[18] M.A. Abdel Rasoul, G.I.Kh. Marei, Samir A.M. Abdelgaleil, Evaluation of antibacterial properties and biochemical effects of monoterpenes on plant pathogenic bacteria, Afr. J. Microbiol. Res. 6 (15) (2012) 3667–3672, https://doi.org/10.5897/AJMR12.118.

[19] M.F. Lopez, C. Cano-Ramirez, M. Shibayama, G. Zuniga, Pinene and myrcene induce ultrastructural changes in the midgut of *Dendroctonus valens* (Coleoptera: Curculionidae: Scolytinae), Ann. Entomol. Soc. Am. 104 (3) (2011) 553–561, https://doi.org/10.1603/AN10023.

[20] http://www.hmdb.ca/metabolites/HMDB0038169.

[21] J.T. Davies, E.K. Rideal, Interfacial Phenomena, Academic Press, New York/London, 1963.

[22] L. Ter Minassian-Saraga, Recent work on spread monolayers, adsorption and desorption, J. Colloid Interface Sci. 11 (1956) 398–418. https://doi.org/10.1016/0095-8522(56)90157-X.

[23] M. Broniatowski, M. Flasiński, P. Wydro, Lupane-type pentacyclic triterpenes in Langmuir monolayers: a synchrotron radiation scattering study, Langmuir 28 (2012) 5201–5210, https://doi.org/10.1021/la300024f.

[24] M. Broniatowski, M. Flasiński, P. Wydro, P. Fontaine, Grazing incidence diffraction studies of the interactions between ursane-type antimicrobial triterpenes and bacterial anionic phospholipids, Colloids Surf. B: Biointerfaces 128 (2015) 561–567, https://doi.org/10.1016/j.colsurfb.2015.03.009.

[25] K. Kjaer, Some simple ideas on X-ray reflection and grazing-incidence diffraction from thin surfactant film, Physica B 98 (1994) 100–109, https://doi.org/10.1016/0921-4526(94)90137-6.

[26] J. Als-Nielsen, D. Jacquemain, K. Kjaer, F. Leveiller, M. Lahav, L. Leiserowitz, Principles and applications of grazing incidence X-ray and neutron scattering from ordered molecular monolayers at the air-water interface, Physics Rep. 246 (1994) 251–313, https://doi.org/10.1016/0370-1573(94)90046-9.

[27] L. Qiao, A. Ge, Y. Liang, S. Ye, Oxidative degradation of the monolayer of 1-Palmitoyl-2-Oleoyl-sn-Glycero-3-Phosphocholine (POPC) in low-level ozone, J. Phys. Chem. B 119 (2015) 14188–14199, https://doi.org/10.1021/acs.jpcb.5b08985.

[28] C. Böhm, H. Möhwald, L. Leiserowitz, J. Als-Nielsen, K. Kjaer, Influence of chirality on the structure of phospholipid monolayers, Biophys. J. 64 (1993) 553–559, https://doi.org/10.1016/S0006-3495(93)81386-9.

[29] M.P. Krafft, F. Giulieri, P. Fontaine, M. Goldmann, Reversible stepwise formation of mono- and bilayers of a fluorocarbon/hydrocarbon diblock on top of a phospholipid Langmuir monolayer. A case of vertical phase separation, Langmuir 17 (2001) 6577–6584, https://doi.org/10.1021/la010587a.

[30] P. Wydro, M. Flasiński, M. Broniatowski, Molecular organization of bacterial membrane lipids in mixed systems—a comprehensive monolayer study combined with grazing incidence X-ray diffraction and Brewster–angle microscopy experiments, Biochim. Biophys. Acta 1818 (2012) 1745–1754, https://doi.org/10.1016/j.bbamem.2012.03.010.

[31] E. Maltseva, A. Kerth, A. Blume, H. Mohwald, G. Brezesinski, Adsorption of amyloid β (1–40) peptide at phospholipid monolayers, ChemBioChem 6 (2005) 1817–1824, https://doi.org/10.1002/cbic.200500116.

[32] G. Wu, J. Majewski, C. Ege, K. Kjaer, M.J. Weygand, K.J.C. Lee, Interaction between lipid monolayers and Poloxamer 188: an X-ray reflectivity and diffraction study, Biophys. J. 89 (2005) 3159–3173, https://doi.org/10.1529/biophysj.104.052290.

[33] E. Maltseva, V.L. Shapovalov, H. Mohwald, G. Brezesinski, Ionization state and structure of L-1,2-dipalmitoylphosphatidylglycerol monolayers at the liquid/air Interface, J. Phys. Chem. B 110 (2006) 919–926, https://doi.org/10.1021/jp0555697.

[34] M. Flasiński, M. Gawryś, M. Broniatowski, P. Wydro, Studies on the interactions between parabens and lipid membrane components in monolayers at the air/aqueous solution interface, Biochim. Biophys. Acta 1858 (2016) 836–844, https://doi.org/10.1016/j.bbamem.2016.01.002.

[35] S.W. Barton, B.N. Thomas, E.B. Flom, S.A. Rice, B. Lin, J.B. Peng, J.B. Ketterson, P. Dutta, X-ray diffraction study of a Langmuir monolayer of $C_{21}H_{43}OH$, J. Chem. Phys. 89 (1988) 2257–2270, https://doi.org/10.1063/1.455068.